Energy Proceedings
Vol 49, 2024
ISSN 2004-2965

Effect of Reynolds Number on Combustion Stability and Flame Macrostructure in a Dual Annular Combustor#

Md. Imteaz Ahmed[1], Qazi Talal[1], Esmail M. A. Mokheimer[1,2*]
1 Mechanical Engineering Department, King Fahd University of Petroleum & Minerals, Dhahran, Saudi Arabia
2 Interdisciplinary Research Center for Sustainable Energy Systems (IRC-SES), King Fahd University of Petroleum & Minerals, Dhahran, Saudi Arabia
(*Corresponding Author: esmailm@kfupm.edu.sa)

ABSTRACT

This study was conducted to investigate the impact of Reynolds number on combustion stability and flame macrostructure in a dual annulus stratified swirl burner. Stratified burners are known for their lower NOx and increased flame stability, but their stability also depends on combustor geometry, stratification ratio, equivalence ratio, and flow dynamics. The study revealed that flame static stability decreases with increasing Reynolds number. The flame blowout equivalence ratio increases by 11.6% as Reynolds number increases from 1000 to 3500 which was due to low vortical temperature with less residence time in the recirculation zone. Flame macrostructure also revealed that at lower Reynolds numbers, the flame stabilizes at inner and central shear layers, while at higher Reynolds numbers, it stabilizes at only central shear layer. Thermoacoustic instability is not observed at lower Reynolds numbers up to 2000, but thermoacoustic instability is observed at higher Reynolds numbers of 2500 and above. An interesting phenomenon of beating oscillation was observed at 2500 Reynolds number at stoichiometric conditions.

Keywords: Stratified Burner, Thermoacoustic instability, Static stability, Flame macrostructure, Effect of Reynolds number, Beating oscillation

NONMENCLATURE

Abbreviations	
LBO	Lean Blowout
SR	Stratification ratio
PMT	Photomultiplier Tube
FFT	Fast Fourier Transform
Symbols	
Φ_g	Global equivalence ratio
Re	Reynolds Number

1. INTRODUCTION

The International Energy Agency (IEA) reports an increasing energy consumption across various sectors, with total energy demands reaching 442 EJ in 2023 [1]. Fuel combustion is crucial to meet these demands but produces significant environmental impacts [2]. Lean premixed combustion offers a solution to mitigate these emissions but faces challenges in stability, such as blowout and thermoacoustic instabilities, which can lead to hazardous incidents [3]. Effectively regulating combustion stability and emissions are crucial for the successful implementation of novel burners in both small and large-scale energy conversion systems that employ gas turbines, furnaces, boilers (steam generators), etc. Improved stability leads to more efficient and safer operation in such applications. Controlling the instability also reduces the high-amplitude cyclic mechanical loads and prevents the failure of mechanical components in gas turbine power plants [4]. The use of swirlers enhances flame stability by improving fuel and oxidizer mixing, resulting in improved combustion and lean blowout limit. The stratified burner uses two inlets for premixed fuel and air at different local equivalence ratios. Stratified premixed burner displays greater stability with lower NOx emissions. This parameter affects stability and the emissions from stratified flames as they affect the flame propagation speed and the entire flame-flow interactions [5].

The stratified flame propagation, as observed by Kang and Kyritsis [6], significantly enhances the prediction of flame speed, incorporating local equivalence ratio and spatial gradient values, while Pasquier et al. [7] also discovered similar findings in experimental studies on propane and air flame propagation. The stratified burner has been developed and tested in many laboratories to observe its behavior. Several burners, including the BASIS burner [8], the

This is a paper for the 16th International Conference on Applied Energy (ICAE2024), Sep. 1-5, 2024, Niigata, Japan.

Cambridge slot burner [9], Cambridge Stratified burner [10], the Oracle burner [11], the Darmstadt burner [12], and the Sydney inhomogeneous pilot burner [13] have been thoroughly examined via numerical and experimental studies. The influence of stratification on flame stability, emissions, and macrostructure temperature shows improved results.

Sweeney et al. [14] studied stratified flames composition, finding greater surface density and scalar dissipation compared to premixed flames. However, higher turbulence showed negligible dependency on surface density, curvature, and scalar dissipation. Han et al. [15] investigated thermoacoustic instabilities and flame macrostructures of stratified swirling flames, observing distinctive flame forms and flame fluctuation being more susceptible to stratification ratio.

The Reynolds number can enhance flame stability in gas turbine combustors. Wang et al. [16] examined experimentally and numerically LBO performance with Reynolds number. The findings demonstrated a drop in the fuel-air ratio as the inlet Reynolds number increased, highlighting the significant influence of the inlet Reynolds number on the LBO. Yoon et al. [17] studied the impact of fuel-air mixture velocity in a gas turbine combustor and revealed that instability occurred at 30 and 70 m/s, while 50 m/s conditions remained stable. At 30 m/s, phase changes caused flame-intensity variations, while at 50 m/s, flame length and intensity remained stable. However, at 70 m/s significant flame structure was observed where heat release intensity oscillation and outer recirculation zone contributed to flame stabilization. Junjie Chen's [18] study on inlet velocity in millimeter-scale combustion systems revealed its critical role in flame stability, with a narrow optimal range for sustained combustion. Design recommendations were provided based on these findings. Thus, this opens the scope to investigate the effect of Reynolds number with stratification to find the alteration in flame macrostructure as well as in combustion instability. The effect of using a swirler in this study will also provide a new dimension to investigate. In this aspect, a dual annulus burner has been designed and manufactured. Swirler can be incorporated with the annulus for the swirling effect. In this work, the effect of Reynolds number in a stratified swirl burner has been studied. The result has been discussed and presented here.

2. METHODOLOGY

2.1 Experimental Setup

Figure 1 illustrates the schematic layout of the experimental apparatus employed for methane-air

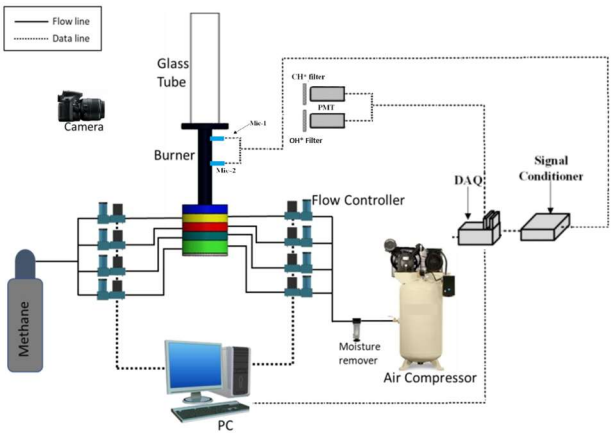

Fig. 1 Schematic diagram of experimental setup

combustion. Air is acquired from a compressor and subsequently passed through a moisture removal device to eliminate the water vapor present in the air. A compressed gas cylinder was utilized to supply high-purity methane of grade N4.5 (99.995%) as fuel. The gases have passed through stainless steel conduits. The pipes are directly connected to the plenum of the burner, where the air and fuel are mixed before traveling downstream into the combustion chamber.

ALICAT mass flow regulators are employed to govern the flow of the reactants from their respective sources to the combustor. The mass flow controllers have a reading accuracy of ±0.8% and a scale accuracy of ±0.2%. The Flow Vision application has been employed to digitally set up the mass flow controller. The mass flow controller can be manually configured using its mini-LED screen and buttons. To analyze the macrostructure of the flame, images of the flame were taken using a Nikon D5200 camera. The period of exposure, ISO sensitivity, and aperture settings were important factors in acquiring high-quality photographs for analytical purposes. The camera used a 1/3 second exposure duration, ISO 1000 sensitivity, and an aperture of f/1.8.

2.2 Combustor Details

Figure 2 depicts the schematic layout of the stratified dual annulus swirl burner utilized in the experimental study. The burner is formed of three cylindrical tubes that are placed concentrically, resulting in a double-annular shape. The image depicts the dimensions of the outer cylindrical tube, with a diameter of 38.10 mm and a thickness of 1.50 mm. The central circular tube has an inner diameter of 23 mm and a width of 2.40 mm. The

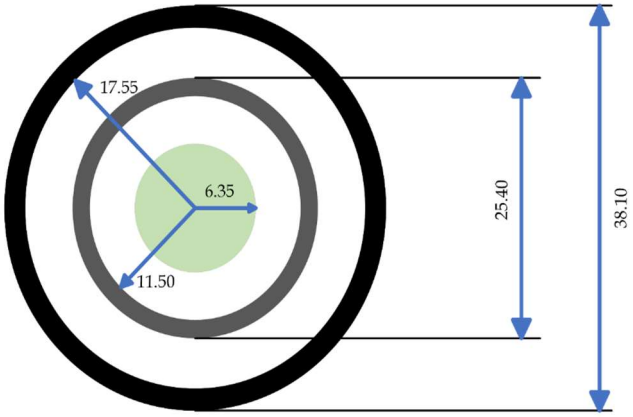

Fig. 2 Detailed geometry of dual annulus stratified swirl combustor

inner circle made completely of ceramic, has a radius of 6.35 mm. The innermost tube will be devoid of any flow source and is designed to serve as a bluff body. The ceramic cap holds firmly to maintain a flame in position. The circulation of flow through the concentric tubes is aided by four plenums, with each annulus being supplied by two of the four plenums. Additional length has been added to support a fully developed flow. Two swirlers were employed in this experiment to induce a swirling motion in the fuel and air supply within the line. The swirling vents are inclined at a 30-degree angle relative to the horizontal axis. The radial swirler is made up of a total of 8 holes, each measuring 2.5 mm in diameter.

2.3 Instrumentation & Operating Condition

This experiment entails the use of a microphone to monitor sound pressure, a digital camera with a CH* bandpass filter to analyze the macro flame structure filter, and an analysis of heat release fluctuation from a PMT using OH* and CH* filters. A pair of high-end microphones (MIC-093) were used to measure the sound signal. These two microphones exhibit significant levels of intensity and are manufactured by Kulite Semiconductor Products Inc. Figure 1 illustrates the exact positioning of the microphone. The first microphone is situated 50 mm in front of the combustor plane, whilst the second microphone is positioned 90 mm in front of the combustor plane. The technique of flush mounting has been used in the outer annulus.

The fluctuations in heat release within the flame can be measured and visualized using chemiluminescence intensities generated by intermediate radicals like CH* and OH*. This experiment utilized two photomultiplier tube modules (PMT), namely of the H10722-110 type manufactured by Hamamatsu Photonics UK LTD, to capture both OH* and CH* chemiluminescence. The PMTs are utilized in combination with OH* and CH* bandpass filters. The PMT and filters are situated at a consistent distance to precisely record the configuration of the flame. The OH* filter exhibits peak transmission at a wavelength of 308 ±5 nm, while the CH* filter demonstrates peak transmission at a wavelength of 430±5 nm. These filters have been manufactured by Thorlabs. The data-collecting device of National Instruments (NI) is used to capture sound pressure and heat release measurements, which are then recorded using LABVIEW software. The data was collected at a sampling frequency of 5 kilohertz over 10 seconds, resulting in a total of 50,000 data points captured for each situation. The experiments are conducted under ambient air pressure and normal room temperature settings. The obtained data undergoes spectral analysis using the Fast Fourier Transform (FFT) to convert it from the time domain to the frequency domain. The purpose of this experiment is to study the effect that variations in Reynolds number have on flame stability, specifically regarding both thermoacoustic and static stability. The Reynolds number will vary between 1000 and 3500 when the global equivalency ratio shifts from lean to rich. The swirler will be employed to enhance the flow's stability. With a stratification ratio (SR) of 1, the outer Reynolds number was twice the inner Reynolds number. The inner Reynolds number was changed from 1000 to 3500, continuing up by 500 each time.

3. RESULTS AND DISCUSSION

3.1 Static Stability

A combustor can only sustain a stable flame within a specific range of air/fuel ratios [19]. The blowout or extinction of flame events is determined by the properties of the fuel and oxidizer, the speed of the flow, and the structure of the burner [20]. The point at which flame blowout or extinction occurs is commonly known as the weak extinction limit or Lean Blowout limit (LBO). A higher Lean Blowout (LBO) typically corresponds to a lower equivalence ratio at which the flame blows off.

The objective of this research was to determine the global equivalence ratio at which blowout/blowoff occurs by varying the inner Reynolds number. Changes in the global equivalence ratio resulted in a change in the power of the combustor. The results are shown in terms of Re_{in}, varying from 1000 to 3500. At a stratification

ratio (SR) of 1, flame blowout occurs at a global equivalence ratio (ϕ_g) of approximately 0.45 with slight variation as Reynolds number changes. As the inner Reynolds number increases, the LBO limit decreases. From Rein=1000 to Rein=3500, the value of ϕ_g increasing from 0.43 to 0.48. This is due to the presence of larger vortices at higher flow velocity which reduces the vortical temperature [21] and the extinction strain rate, causing blowout at a higher equivalence ratio [22]. In Lefebvre's work [23-24], similar results have been reported which indicated that with increasing velocity LBO limit has decreased.

3.2 Flame Macrostructure

Investigating the macrostructures of flames offers valuable information regarding the process of flame extinguishment. Furthermore, it aids in determining the anchoring location and total duration of combustion, which may be advantageous in the design of combustors [25]. The flame microstructure has been recorded using a digital camera equipped with a CH* filter. Figure 3 shows a comparative schematic diagram of W and V shape flames with their anchoring position.

At Reynolds numbers of 2000, A and B represent the flame anchoring positions for the W shape flame. The flame root B is stabilized at the bluff body in between

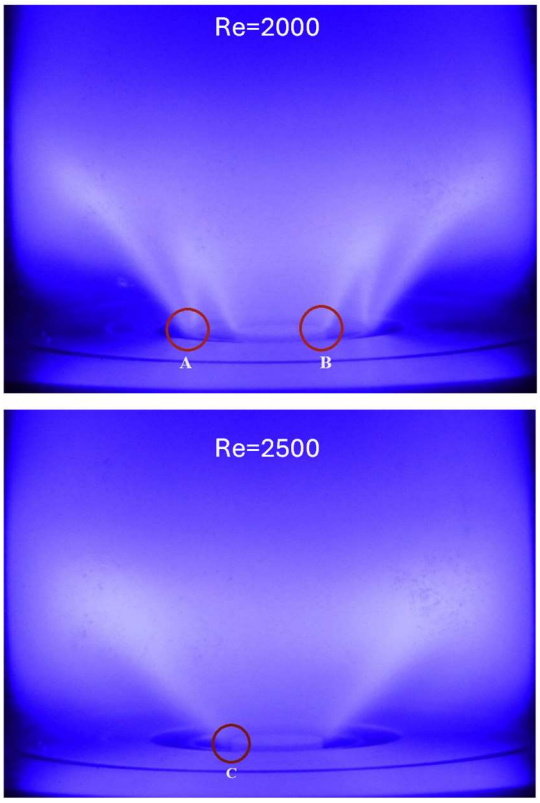

Fig. 3 Flame macrostructure comparing W (Re=2000) and V (Re=2500) shape flame at φ_g=1

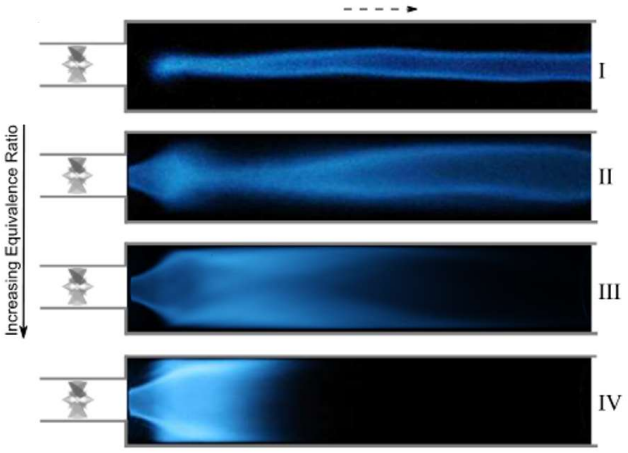

Fig. 4 Conventional Swirl flame shapes [26]

central recirculation zone (CRZ) and center shear layer (CSL). Flame root A stabilizes on the top of the inner tube in between inner shear layer (ISL) and outer recirculation zone (ORZ). Thus, a resulting flame shape resembling the letter 'W' is formed. At Reynolds number Re_{in}=2500, the flame at ϕ_g=1 doesn't show any W flame structure rather it forms V shape flame represented by C in the figure 3. The V shape flame stabilizes at CSL in between the CRZ and ORZ.

Figure 4 demonstrates conventional swirl flame shapes [26]. Most of these studies reported the swirling flame macrostructures is characterized by four shapes: a columnar tubular flame (Type-I); an bubble-columnar flame (Type-II); a single conical flame stabilized along the inner shear layer ISL (Type-III can be seen as V shape); and a double conical flame with an additional flame front stabilized in the ORZ and along the outer shear layer OSL (Type-IV can sometimes form M/W shape). These flames can be lifted or attached to the center body and/or sudden expansion along the side wall. The flame type generally transitions from Type-IV to Type-I as the equivalence ratio decreases leading towards blowout.

Figure 5 illustrates the flame structures at Reynolds number of Re_{in}=2000 and Re_{in}=2500 for a swirling flame with a stratification ratio of 1 for varying equivalence ratio (blowout to stoichiometric condition). At Reynolds number 2000, at stoichiometric condition, the Type-IV W-shape flame has been observed. This W shape flame continues up to ϕ_g=0.9. After that the flame transitions to central shear layer V flame of Type-III with extended flame front which continues up to ϕ_g=0.6. After this point, the flame becomes unstable, and a long bubble columnar flame of Type-II is observed. It eventually blows off, following the same pattern as a conventional swirl flame going from Type IV to Type I before extinguishing.

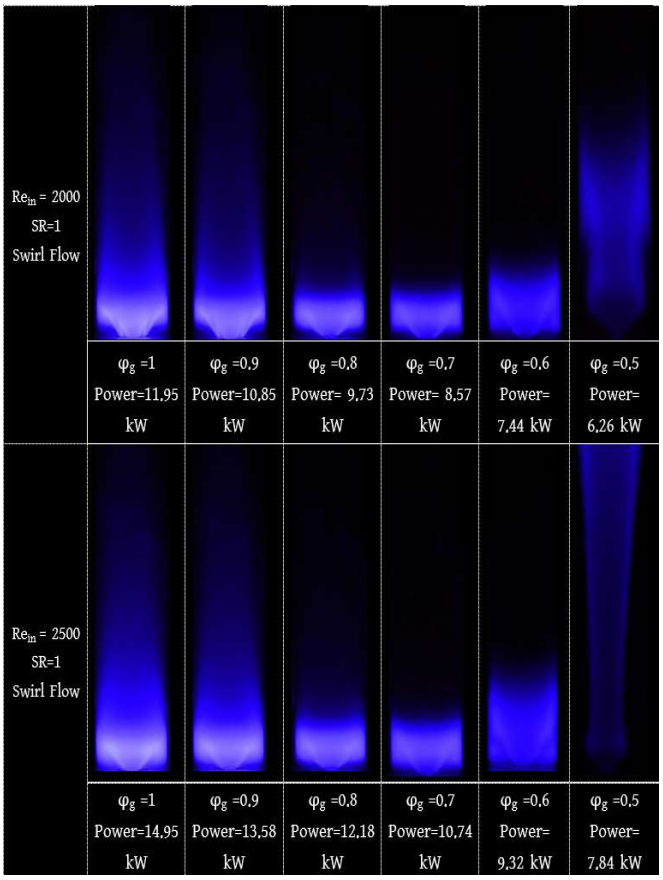

Fig. 5 Flame macrostructure at different Reynold number at different equivalence ratio

For Reynolds number Re_{in}=2500, the flame at rich condition (ϕ_g=1-0.9) doesn't show any W shape structure rather it forms Type III V shape with extended flame front. This V-shaped flame dominates up to ϕ_g=0.6 although the intensity of the flame has been reduced as well as the power. Lastly at ϕ_g=0.5, the long column shape flame Type I appeared which represents unstable flame and eventually blows out after that.

Furthermore, a detailed flame macrostructure study has been done for a range of 1000-3500 Reynolds numbers which can be addressed in the extended report.

3.3 Thermoacoustic Instability

Swirling flames are investigated at varying equivalence ratios to identify thermoacoustic instability followed by peak amplitude and frequencies. For this investigation, 2 microphone signals to record the sound pressure and two filters (one CH* & one OH*) with PMT have been used to capture the heat release fluctuation. When any of the peaks recorded by the microphones coincide with the peaks recorded by PMT's at identical frequency, thermoacoustic instability triggers at those frequencies in the dual annular burner.

At Reynolds numbers 2000, there was no occurrence of coinciding peaks, indicating the absence of thermoacoustic instabilities. No peak amplitudes at any frequency were recorded by either the microphones or the PMTs for this case. As there was an absence of any peak in the sound pressure spectrum as well as heat release spectra, there was no occurrence of an onset or coupling that may lead to thermoacoustic instability.

Therefore, no image has been depicted to show any signal of sound pressure and heat release spectra under these situations. The stratified burner can be operated without any concern of thermoacoustic instability in all ranges of equivalence ratio at 2000 inner Reynolds number.

However, the situation is different at Reynolds number 2500 as the acoustics pressure spectra and heat release spectra indicate the onset condition for thermoacoustic instability for ϕ_g= 0.8-1.10 shown in Figure 6. At ϕ_g= 0.75, the sound pressure peak frequency had a minor amplitude, but no significant peak or amplitude was found in the heat release spectra. This demonstrated that no instability had been recorded. At ϕ_g=0.8, both the sound pressure recorded by microphone Mic-1 and the heat release spectra from the CH*- PMT revealed the beginning of thermoacoustic instabilities, with a peak frequency of 478.9 Hz. The pressure and heat release spectra exhibit coupling at 489.4 Hz at ϕg=0.85. Following the coupling, thermoacoustic instabilities are amplified, leading to somewhat greater amplitude peaks in both spectra. Both spectra show a rightward shift at ϕ_g=0.9, with a peak frequency of 500.5 Hz. The highest peak amplitude for sound by the microphone was recorded at this condition with a magnitude of 0.009551 which when converted was approximately 160 dB. At that time, the experiment is distinguished by an excessive amount of physical noise, which was very uncomfortable and unpleasant. This high intensity noise remains until 0.95 and at this condition reaches its maximum amplitude value of 0.00062 A.U. in heat release spectra at 502.8 Hz.

At ϕ_g=1, there is a considerable drop in heat release spectra amplitude and sound pressure amplitude, however, the frequency illustrates a rapid shift from 500 Hz to around 700 Hz. An interesting phenomenon called beating oscillation also occurred at this stoichiometric condition. The beating frequencies are 716 and 725 Hz. Despite the significantly smaller amplitudes of the sound pressure and heat release spectra compared to ϕ_g=0.9, the presence of beating oscillation caused thermoacoustic instability at both frequencies. According to the literature, beating occurs due to a

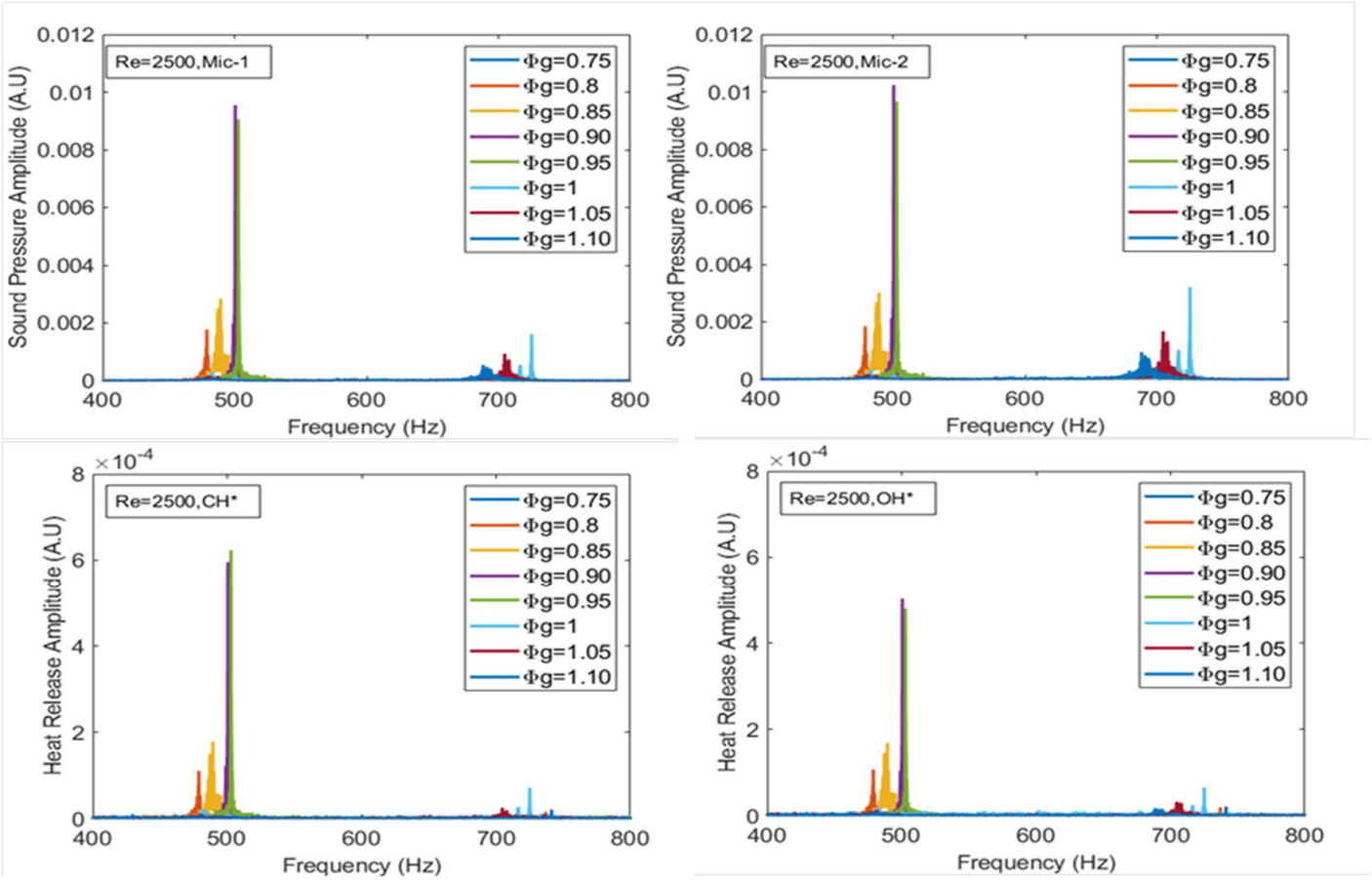

Fig. 6 Acoustic pressure spectra and heat release spectra (CH & OH*) at Reynolds number Re=2500 for swirl flames*

difference in cycle times between the main and pilot flames [27]. Han et al. [28] also reported the presence of beating phenomena. Under stoichiometric conditions, the coupling progresses to extremely low amplitude coupling before decoupling under rich conditions with an equivalence ratio of 1.15. At stoichiometric conditions, the maximum frequency has been reached which is 725 Hz. Thermoacoustic instability is reported at frequencies ranging from 450 Hz to 750 Hz with variable amplitudes.

Evaluating the data from the second microphone positioned at 90 mm upstream illustrated slightly higher amplitudes for all cases as can be observed from figure 6. For the 2nd PMT with the OH* filter, in the heat release spectra, the amplitude of the OH*-PMT peak is lower than that of the CH*-PMT. All the peaks, however, occur at identical frequencies in all 4 spectra.

Further analysis has been conducted for a range of Reynolds numbers from 1000-3500 with regards to thermoacoustic instability. To further strengthen the instability study, phase space reconstruction and flame transfer function have also been analyzed. This along with the emission analysis was also carried out for this particular study and will be reported in the extended version of the paper.

4. CONCLUSIONS

The combustion stabilities- (static and thermoacoustic) with flame macrostructure at different Reynolds numbers for lean to rich fuel equivalence ratio in a dual annulus stratified swirl burner have been investigated during this work. Static stability study shows that the Lean Blowout limit-LBO decreases with increasing Reynolds number from 1000 to 3500 due to low vortical temperature with less residence time which extinguishes the flame at a higher equivalence ratio.

The flame macrostructure is significantly affected by Reynolds number. At a low Reynolds number of 2000, the flame structure was stabilized on both the inner shear layer and central shear layer forming a W shape flame while at a Reynolds number of 2500, the flame stabilized in the inner shear layer only forming V shape flame for fuel rich condition. Thermoacoustic instability was also observed at the higher Reynolds number of 2500 while there was no thermoacoustic instability at Re_{in}=2000. Furthermore, beating oscillation was also observed at stoichiometric condition.

ACKNOWLEDGMENT

The authors would also like to acknowledge the research support provided by DROC and the Renewable Energy Technical Incubator (RETI) funded by the National Industrial Development and Logistics Program (NIDLP) under the Interdisciplinary Research Center for Sustainable Energy Systems (IRC-SES) at King Fahd University of Petroleum & Minerals, through Project No. CREP2522 and INRE2409.

DECLARATION OF INTEREST STATEMENT

The authors declare that they have no known competing financial interests or personal relationships that could have appeared to influence the work reported in this paper. All authors read and approved the final manuscript.

REFERENCE

[1] IEA (2023), World Energy Outlook 2023, IEA, Paris https://www.iea.org/reports/world-energy-outlook-2023, Licence: CC BY 4.0 (report); CC BY NC SA 4.0 (Annex A).

[2] Mikulčić, H., Baleta, J., Wang, X., Wang, J., Qi, F., & Wang, F. (2021). Numerical simulation of ammonia/methane/air combustion using reduced chemical kinetics models. International Journal of Hydrogen Energy, 46(45),23548–23563. https://doi.org/10.1016/j.ijhydene.2021.01.109

[3] Chu, H., Huang, Z., Zhang, Z., Yan, X., Qiu, B., & Xu, N. (2024). Integration of carbon emission reduction policies and technologies: Research progress on carbon capture, utilization and storage technologies. Separation and Purification Technology,343,127153. https://doi.org/https://doi.org/10.1016/j.seppur.2024.127153

[4] Altunlu, A. C. (2013). The analysis of mechanical integrity in gas turbine engines subjected to combustion instabilities. [PhD Thesis - Research UT, graduation UT, University of Twente]. University of Twente. https://doi.org/10.3990/1.9789036500555

[5] Anselmo-filho, P., Hochgreb, S., Barlow, R. S., & Cant, R. S. (2009). Experimental measurements of geometric properties of turbulent stratified flames. Proceedings of the Combustion Institute,32(2),1763–1770. https://doi.org/10.1016/j.proci.2008.05.085

[6] Kang T, Kyritsis DC. Theoretical investigation of flame propagation through compositionally stratified methane-air mixtures. Combustion Theory and Modelling 2009;13:705–19. https://doi.org/10.1080/13647830903093765.

[7] Pasquier N, Lecordier B, Trinité M, Cessou A. An experimental investigation of flame propagation through a turbulent stratified mixture. Proceedings of the Combustion Institute2007;31I:1567–74. https://doi.org/10.1016/j.proci.2006.07.118.

[8] Han, X, Laera, D., Morgans, A. S., Sung, C. J., Hui, X., & Lin, Y. Z.(2019). Flame macrostructures and thermoacoustic instabilities in stratified swirling flames. Proceedings of the Combustion Institute, 37(4), 5377–5384. https://doi.org/10.1016/j.proci.2018.06.147

[9] Barlow RS, Wang GH, Anselmo-Filho P, Sweeney MS, Hochgreb S. Application of Raman/Rayleigh/LIF diagnostics in turbulent stratified flames. Proceedings of the Combustion Institute 2009;32 I:945–53. https://doi.org/10.1016/j.proci.2008.06.070.

[10] Sweeney, M. S., Hochgreb, S., Dunn, M. J., & Barlow, R. S. (2012). The structure of turbulent stratified and premixed methane / air flames I : Non-swirling flows. Combustion and Flame, 159(9), 2896–2911. https://doi.org/10.1016/j.combustflame.2012.06.001

[11] Ribert G, Champion M, Gicquel O, Darabiha N, Veynante D. Modeling nonadiabatic turbulent premixed reactive flows including tabulated chemistry. Combustion and Flame 2005;141:27180.https://doi.org/10.1016/j.combustflame.2004.12.019.

[12] Arndt CM, Severin M, Dem C, Stöhr M, Steinberg AM, Meier W. Experimental analysis of thermo-acoustic instabilities in a generic gas turbine combustor by phase-correlated PIV, chemiluminescence, and laser Raman scattering measurements. Experiments in Fluids 2015;56:1–23. https://doi.org/10.1007/s00348-015-1929-3.

[13] Meares S, Masri AR. A modified piloted burner for stabilizing turbulent flames of inhomogeneous mixtures. Combustion and Flame 2014;161:484–95. https://doi.org/10.1016/j.combustflame.2013.09.016.

[14] Sweeney MS, Hochgreb S, Dunn MJ, Barlow RS. The structure of turbulent stratified and premixed methane/air flames II: Swirling flows. Combustion and Flame 2012;159:2912–29. https://doi.org/10.1016/j.combustflame.2012.05.014.

[15] Han X, Laera D, Yang D, Zhang C, Wang J, Hui X, et al. Flame interactions in a stratified swirl burner : Flame stabilization , combustion instabilities and beating oscillations. Combust Flame 2020;212:500–9. https://doi.org/10.1016/j.combustflame.2019.11.020

[16] Wang, C., Liu, W., Bi, Z., Li, G., & Zeng, W. (2023). Experimental and numerical prediction of LBO performance in a centrally staged combustor. Applied Thermal Engineering, 227(December 2022), 120431.

https://doi.org/10.1016/j.applthermaleng.2023.120431
[17] Yoon, J., Kim, M., Hwang, J., Lee, J., & Yoon, Y. (2013). Effect of fuel e air mixture velocity on combustion instability of a model gas turbine combustor. Applied Thermal Engineering, 54(1), 92–101. https://doi.org/10.1016/j.applthermaleng.2013.01.032
[18] Chen, J. (2022). Effect of inlet velocity on the combustion characteristics of a methane-air mixture in a millimeter-scale system with cavity flame stabilization. https://doi.org/10.21203/rs.3.rs-1699851/v1
[19] Sloan, D. G. (2016). Design and Development of a Research Combustor for Lean Blow-Out Studies. 114(January 1992), 13–19.
[20] Moore, N. J., Mccraw, J. L., & Lyons, K. M. (2008). Observations on Jet-Flame Blowout. 2008. https://doi.org/10.1155/2008/461059
[21] Zukoski EE, Marble FE. Experiments Concerning the Mechanism of Flame Blowoff From Bluff Bodies. Proceedings of the Gas Dynamics Symposium on Aerothermochemistry 1956:205–2010.
[22] Nair S, Lieuwen T. Near-blowoff dynamics of a bluffbody stabilized flame. Journal of Propulsion and Power 2007;23:421–7. https://doi.org/10.2514/1.24650.
[23] Ballal, D. R., & Lefebvre, A. H. (2016). Weak Extinction Limits of Turbulent Flowing Mixtures. 101(78), 343–348.
[24] Baxter, M. R. (2016). Weak Extinction Limits of Large- Scale Fiameholders. 114(October 1992).
[25] Taamallah, S., Shanbhogue, S., & Ghoniem, A. (2016). Turbulent flame stabilization modes in premixed swirl combustion: Physical mechanism and Karlovitz number-based criterion. Combustion and Flame, 166. https://doi.org/10.1016/j.combustflame.2015.12.007
[26] Polytechnique, E., Polytechnique, E., Ghoniem, A. F., Supervisor, T., Hadjiconstantinou, N. G., Science, C., & Abeyaratne, R. (2016). Impact of Fuel and Oxidizer Composition on Premixed Flame Stabilization in Turbulent Swirling Flows : Dynamics and Scaling.
[27] Kim, J., Jang, M., Lee, K., & Masri, A. R. (2019). Experimental study of the beating behavior of thermoacoustic self-excited instabilities in dual swirl combustors. Experimental Thermal and Fluid Science, 105(February), 1–10. https://doi.org/10.1016/j.expthermflusci.2019.03.007
[28] Han X, Laera D, Yang D, Zhang C, Wang J, Hui X, et al. Flame interactions in a stratified swirl burner :Flame stabilization , combustion instabilities and beating oscillations. Combust Flame 2020;212:500–9. https://doi.org/10.1016/j.combustflame.2019.11.020